ACS APPLIED MATERIALS & INTERFACES

Research Article

www.acsami.org

Temperature-Sensitive Fluorescent Organic Nanoparticles with Aggregation-Induced Emission for Long-Term Cellular Tracing

Zhen Wang,† Tu-Ying Yong,† Jiangshan Wan,† Zi-He Li, Hao Zhao, Yanbing Zhao,* Lu Gan,* Xiang-Liang Yang, Hui-Bi Xu, and Chun Zhang*

College of Life Science and Technology, Huazhong University of Science and Technology, and National Engineering Research Center for Nanomedicine, Wuhan, Hubei 430074, China

Supporting Information

ABSTRACT: Temperature-sensitive organic nanoparticles with AIE effect were assembled in water from tetraphenylethene-based poly(*N*-isopropylacrylamide) (TPE-PNIPAM), which was synthesized by ATRP using TPE derivative as initiator. The size and fluorescence of TPE-PNIPAM nanoparticles can be tuned by varying the temperature. These nanoparticles can be internalized readily by HeLa cells and can be used as long-term tracer in live cells to be retained for as long as seven passages.

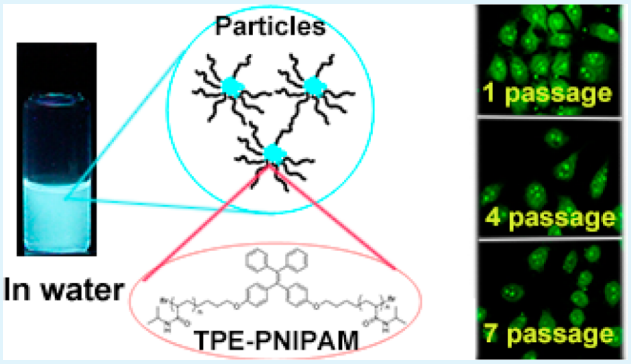

KEYWORDS: *tetraphenylethene (TPE), poly(N-isopropylacrylamide) (PNIPAM), fluorescent organic nanoparticles, aggregation-induced emission (AIE), long-term cellular tracing*

1. INTRODUCTION

Compared with other bioimaging techniques, fluorescent imaging displayed more advantages of high sensitivity, easy operation, and cost-effectiveness.[1−3] Using fluorescent imaging techniques to trace cellular processes over a long period of time is significant for biological or medical researchers because they provide some important information about cell transplantation, migration, division, fusion, and lysis.[4−8] So, development of long-term cellular tracers has attracted great effort in recent years and resulted in different fluorescent probes. For example, quantum dots (QDs), one kind of inorganic nanoparticle, have been used as cellular tracer to stay in cytoplasm for about six generations with high emission and good photostability.[9] However, their heavy metal constituents with potential cytotoxicity limited their application in vivo.[10] In comparison to inorganic QDs, fluorescent organic nanoparticles should be important alternatives because of their ready availability, easy functionality and good biocompatibility.[11−17] However, the fluorescence of organic nanoparticles functionalized from conventional organic fluorophores or conjugated polymers is often weakened or annihilated in the aggregated state because of the aggregation-caused quenching (ACQ) effect.[18] Fortunately, Tang et al. discovered a novel kind of fluorophores with aggregation-induced emission (AIE) properties.[19−21] These AIE fluorogens are nonfluoresent in solutions but become highly fluorescent in aggregation state. So far, different AIE-based organic nanoparticles for application of long-term cellular tracing have been developed by coassembly of AIE molecules with surfactants by multistep procedures. Recently, tetraphenylethene (TPE)[22−31] attached onto chitosan (CS) resulted in TPE-CS bioconjugates, which spontaneously cluster into microparticles inside live cells as long-term cellular tracer.[32] Using different polymers by different synthetic methods to develop novel AIE-based organic nanoparticles undoubtedly afford new opportunities to hunt novel long-term cellular tracers. However, such reports are scattered.[33,34]

Poly(*N*-isopropylacrylamide) (PNIPAM),[35,36] a temperature-sensitive synthetic polymer, undergoes a transition from hydrated coil to dehydrated granule in water at its lower critical solution temperature (LCST) about 32 °C. With the temperature-sensitivity and good biocompatibility, PNIPAMs have been utilized widely in biotechnology, especially in drug delivery systems, temperature-targeted therapy materials, tissue-engineering materials, and so on.[37−39] Recently, we utilized PNIPAM to construct a series of novel drug delivery systems and imaging contrast agent with the temperature-sensitive properties.[40−44]

Herein, we utilized TPE derivative as initiator to synthesize PNIPAM by atom transfer radical polymerization (ATRP). The obtained TPE-PNIPAM (Figure 1) displayed AIE properties and assembled into nanoparticles in water. The size and fluorescence of these TPE-PNIPAM nanoparticles are temper-

Received: December 29, 2014
Accepted: January 20, 2015
Published: January 20, 2015

DOI: 10.1021/am509161y
ACS Appl. Mater. Interfaces 2015, 7, 3420−3425

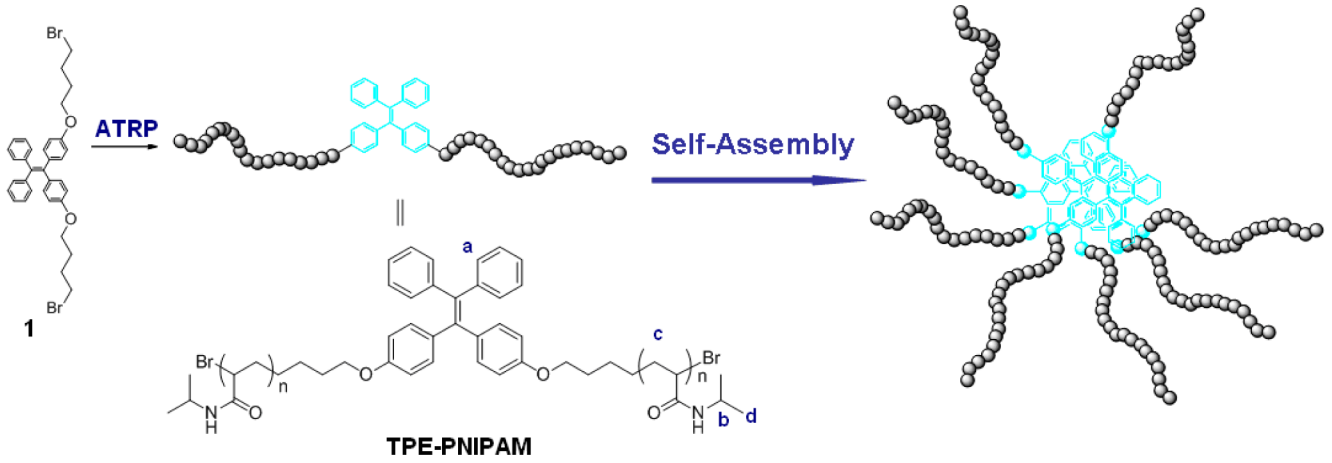

Figure 1. Schematic representation of the formation of nanopaticles from TPE-PNIPAM.

ature-sensitive. Moreover, these TPE-PNIPAM nanoparticles can be readily internalized by HeLa cells and trace the living cells for as long as seven passages.

2. EXPERIMENTAL SECTION

2.1. General Information. Materials obtained commercially were used without further purification. ^{1}H NMR spectra were recorded on a DMX600 NMR. UV spectra were recorded on SHIMADZU UV-2041PC spectrometer. Emission spectra were obtained on HITACHI F-4500 spectrometer. TEM studies were conducted on a Tecnai G220 electron microscope.

2.2. Synthesis of 1. Under argon atmosphere, dihydroxytetraphenylethylene (365 mg, 1 mmol) 1, 4-dibromobutane (648 mg, 3 mmol), and K_2CO_3 (445 mg, 3 mmol) were combined in a 100 mL flask. Acetone (20 mL) was added by syringe. The reaction mixture was refluxed for 10 h and then cooled and partitioned between CH_2Cl_2 (50 mL) and H_2O (40 mL). The resulting mixture was separated, and the aqueous layer was extracted twice with CH_2Cl_2 (20 mL). The combined organics were dried over anhydrous Na_2SO_4, filtered, and concentrated in vacuo. The residue was purified by column chromatography (petroleum ether/CH_2Cl_2, 3/1) to afford **1** as white solid (250 mg, 39.4%). ^{1}H NMR (600 MHz, $CDCl_3$): δ 7.06−7.11 (m, 6H), 7.02 (d, J = 6 Hz, 4H), 6.92 (d, J = 12 Hz, 4H), 6.61 (d, J = 12 Hz, 4H), 3.91 (d, J = 12 Hz, 4H), 3.47 (d, J = 12 Hz, 4H), 2.04 (m, 4H), 1.90 (m, 4H). EI-MS: m/z 634 (M^+). Anal. calcd for $C_{56}H_{50}$: C, 64.37; H, 5.40. Found: C, 64.52; H, 5.26.

2.3. Synthesis of TPE-PNIPAM. Compound **1** (32 mg, 0.05 mmol), *N*-isopropylacrylamide (1.13 g, 10 mmol), DMSO 4 mL and isopropanol (4 mL) were added in a Schlenk tube with a stirrer. The Schlenk tube was frozen with liquid nitrogen for 5 min and degassed via standard freeze−pump−thaw cycles three times. In the thawed state, Me_6TREN (50 μL) was added below the liquid level, the tube was frozen with liquid nitrogen for 5 min, and CuCl (20 mg) was added. The tube was capped, evacuated for 2 min, and backfilled with nitrogen for 5 min. The reaction mixture was stirred at 20 °C for 24 h, dialyzed for 3 days, and then freeze-dried 3 days to give the product (300 mg).

2.4. Cell Culture. Cells of the human cervical carcinoma cell line HeLa were purchased from Type Culture Collection of the Chinese Academy of Sciences (Shanghai, China). The cells were maintained in Dulbecco's modified Eagle's medium (DMEM; Hyclone, Logan, UT) containing 10% fetal bovine serum (FBS, Gibco, Grand Island, NY), penicillin (100 U/mL) and streptomycin (100 μg/mL) at 37 °C in 5% CO_2 in a humidified atmosphere.

2.5. Cytotoxicity Study. HeLa cells were seeded in 96-well plates at a density of 6000 cells/well. After incubation overnight, cells were treated with different concentrations of TPE-PNIPAM for different time courses. The cells were washed with PBS, and then MTT solution (5 mg/mL, 20 μL) was added to the cells in each well. Plates were incubated for an additional 4 h at 37 °C. The medium containing MTT was removed, and dimethyl sulfoxide (DMSO; 150 μL) was added to dissolve the formazan crystals formed by living cells. Absorbance was measured at 488 nm using a Labsystems iEMS microplate reader (Helsinki, Finland).

2.6. Long-Term Cellular Imaging. HeLa cells were seeded in 35 mm cell-culture dishes and incubated overnight. The cells were treated with 100 μg/mL TPE-PNIPAM, washed with phosphate buffered saline (PBS) twice and the image was then taken after 24 h incubation (referred to as the first passage) using Olympus FV1000 confocal microscope (Olympus, Tokyo, Japan) with excitation at 405 nma and emission at 460−480 nm. After that, the cells were collected, and 25% of the cells were transferred to a new dish with fresh cell culture medium. Another image was taken after 48 h incubation (referred to as the second passage). The process was repeated every 2 days and for as long as 7 passages. For quantitative analysis of the intracellular concentration of TPE-PNIPAM, the cells at different passages were harvested and subjected to flow cytometric analysis (FC500, Beckman Coulter, Fullerton, CA).

3. RESULTS AND DISCUSSION

The synthesis of TPE-PNIPAM was depicted as shown in Scheme S1 (Supporting Information). The starting TPE derivative **1** was synthesized by the reaction of dihydroxytetraphenylethylene **2**[31] with 1,4-dibromobutane. This initiator contains two arms for the construction of macromolecule TPE-PNIPAM by ATRP under the catalyst system of CuCl/Me_6TREN in solution of DMSO/*i*-PrOH at room temperature for 24 h. The resultant TPE-PNIPAM was purified by dialysis

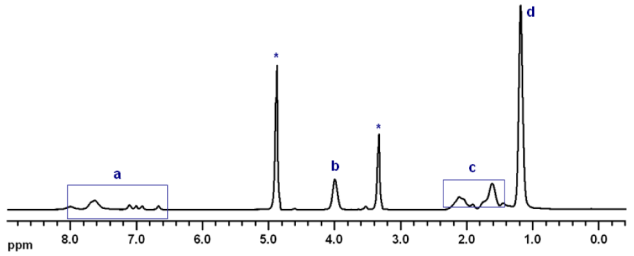

Figure 2. ^{1}H NMR spectrum of TPE- PNIPAM in d_4-MeOH; signals are ascribed to (a) the aromatic protons of the benzyl group, δ = 6.67−8.03 ppm; (b) the methine proton in the isopropyl group, δ = 4.01 ppm; (c) the methylene protons in the backbone, δ = 1.62−2.12 ppm; and (d) the protons of the methyl groups, δ = 1.19 ppm. The solvent and water peaks are noted with asterisks (*).

DOI: 10.1021/am509161y
ACS Appl. Mater. Interfaces 2015, 7, 3420−3425

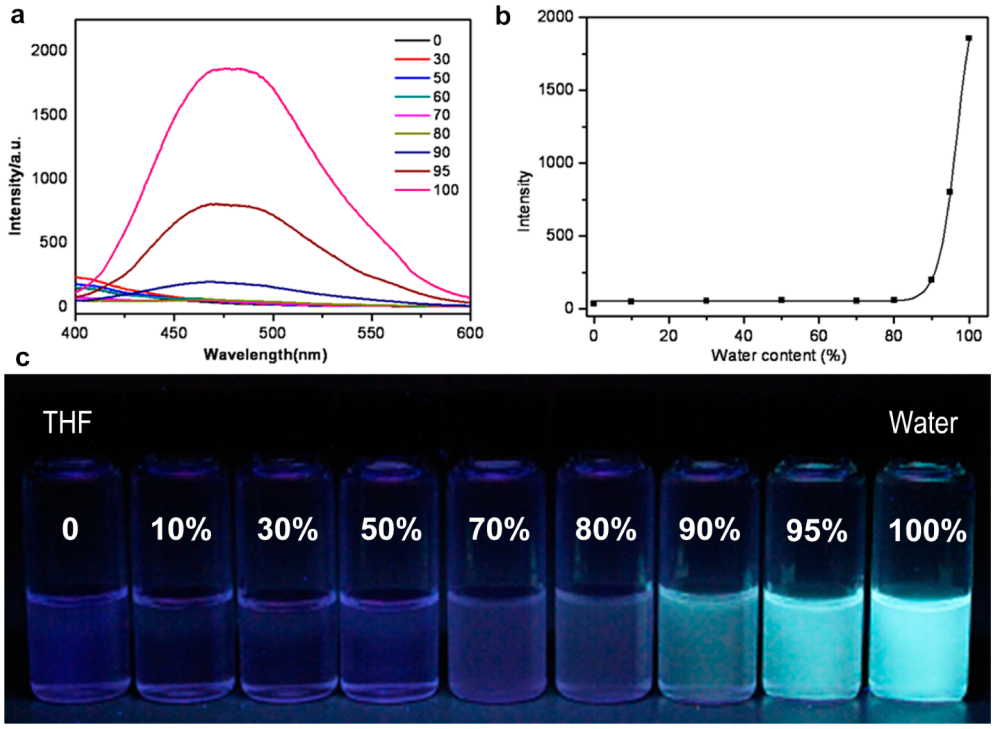

Figure 3. (a) Fluorescent spectra of TPE-PNIPAM in THF/water system with different water contents (320 nm, [TPE-PNIPAM] = 0.5 mg/mL). (b) Change of fluorescent intensity of TPE-PNIPAM in THF/water system at 480 nm. (c) Photographs of TPE-PNIPAM solutions under UV light (365 nm).

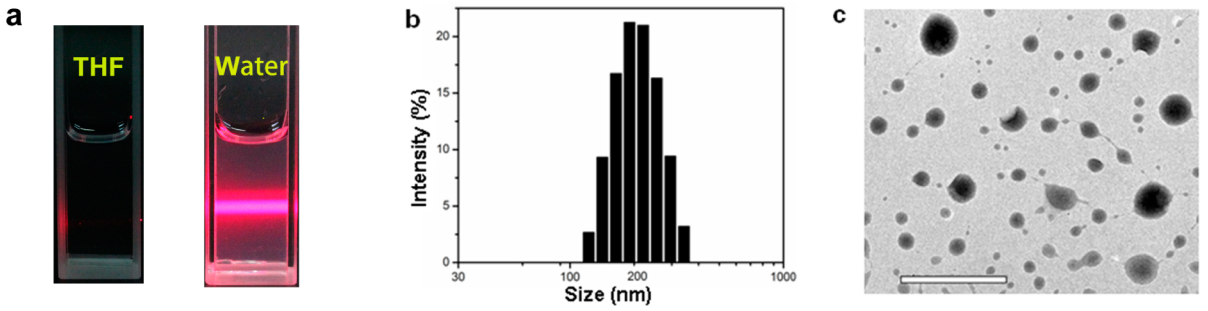

Figure 4. (a) Photographs of TPE-PNIPAM solutions in THF or water under irradiation of laser point. (b) Hydrodynamic size with concentration of 0.5 mg/mL. (c) TEM image of TPE-PNIPAM nanoparticles. Scale bar: 1 μm.

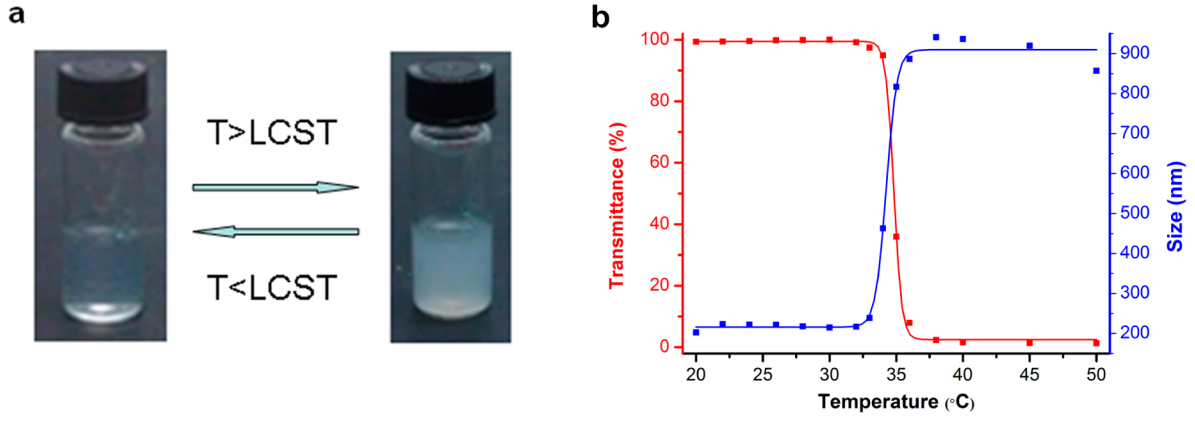

Figure 5. (a) Photographs of TPE-PNIPAM solutions in water at (left) 20 °C and (right) 50 °C. (b, red line) Tansmittance and (blue line) hydrodynamic size vs temperature for TPE-PNIPAM in water (0.5 mg/mL).

in deionized water and characterized by standard spectroscopic methods.

The GPC data indicated that the molecular weight (M_n) of TPE- PNIPAM was 32 kDa with polydispersity index (PDI) of

DOI: 10.1021/am509161y
ACS Appl. Mater. Interfaces 2015, 7, 3420−3425

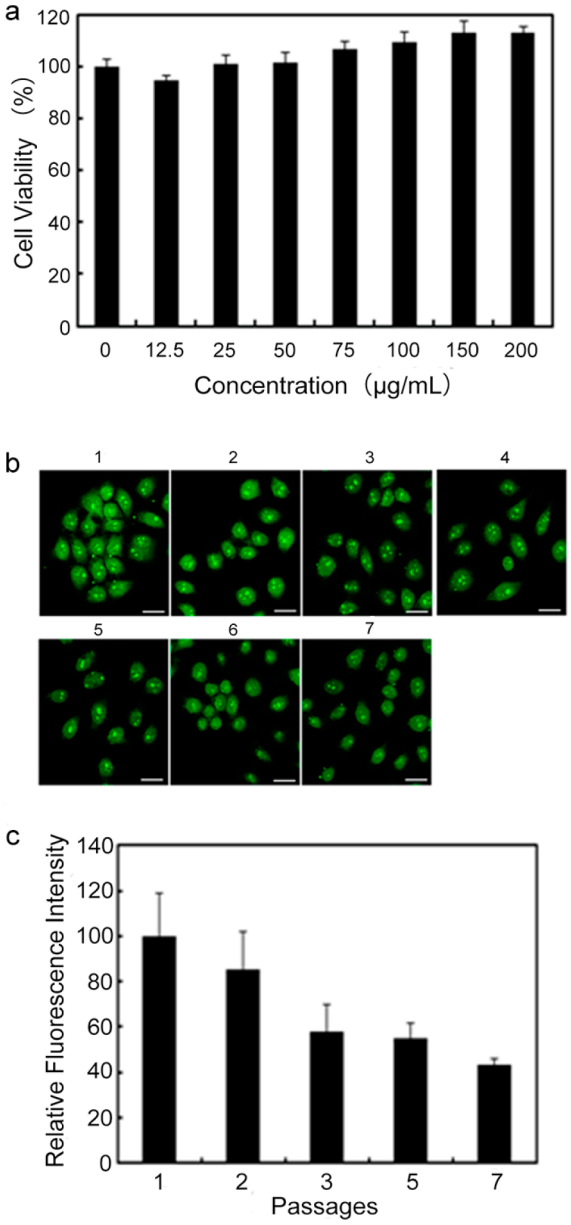

Figure 6. (a) Cell viabilities of HeLa cells treated with different concentrations of TPE-PNIPAM for 48 h by MTT assay. (b) Confocal microscope images of HeLa cells stained with TPE-PNIPAM (100 μg/mL) at different passages. The scale bar is 25 μm. (c) The fluorescence intensity of TPE in HeLa cells stained with TPE-PNIPAM (100 μg/mL) at different passages by flow cytometry. Data as mean values ± SD (n = 3).

1.9. ^{1}H NMR spectrum of TPE-PNIPAM in d4-MeOH is shown in Figure 2. The signals at δ = 6.67−8.03, 4.01, 1.62−2.12, and 1.19 ppm are ascribed to the aromatic protons of the benzyl group, the methine proton in the isopropyl group, the methylene protons in the backbone, and the protons of the methyl groups, respectively. From FT-IR spectrum of the obtained TPE-PNIPAM, we can clearly observe the amide carbonyl stretching band and N−H bending vibration at 1650 and 1548 cm^{-1}, respectively. Combining these results with the results of GPC, ^{1}H NMR, and FT-IR, we can conclude that the formation of TPE-PNIPAM via ATRP is successful.

The AIE properties of TPE-PNIPAM were investigated in THF/water system. As shown in Figure 3, the TPE-PNIPAM was nonemissive at 480 nm when dissolved in THF. When water, the poor solvent for TPE, was added to 90%, the emission became visible. Especially, the fluorescence spectrum displayed a significant enhancement when TPE-PNIPAM was dispersed in pure water. Moreover, the TPE-PNIPAM displayed remarkable photostability, and no obvious fluorescent blenching was observed after irradiated under UV lamp (365 nm) for 0.5 h.

Different with in THF solution, the TPE-PNIPAM can be assembled into nanoparticles in aqueous media with Tyndall effect because of its amphiphilic properties, in which the hydrophobic TPE aggregated in the core and the hydrophilic PNIPAM extended into water at room temperature (Figure 4a). With concentration of 0.5 mg/mL, dynamic light scattering displayed that the hydrodynamic size of these nanoparticles was maintained at ∼200 nm (Figure 4b). Transmission electron microscopy (TEM) experiments displayed the TPE-PNIPAM nanoparticles with a size distribution of 100−300 nm (Figure 4c).

PNIPAM is a well-known thermoresponsive polymer with lower critical solution temperature (LCST) at 32 °C in aqueous media. To investigate the LCST behavior of our TPE-PNIPAM, an aqueous solution of this polymer was heated to 50 °C. Due to the transition from hydrated coil to dehydrated granule of PNIPAM, the transparent solution at room temperature underwent an abrupt change in turbidity when the temperature reached the LCST (Figure 5a). From the results of transmittance and the hydrodynamic size change with temperature, a cloud point of 34 °C was observed, which is consistent with LCST values of other PNIPAM derivatives (∼32 °C; Figure 5b).

The fluorescence change of TPE-PNIPAM with temperature in water was shown in Figure S3 (Supporting Information). The fluorescent intensity decreased with increasing temperature, although a slope change is recorded at 34 °C. In the aggregated nanoparticles of TPE-PNIPAM, increasing temperature quickened the molecular motions and intramolecular rotations and resulted in the continuous decrease in fluorescent intensity, although hydrophobic globulation effects were existent. These similar behaviors could be observed in Tang's **P1b** and **P1c**, the copolymers of TPE with NIPAM.[45]

For the biomedicine application, the cytotoxicity of TPE-PNIPAM was evaluated by the 3-(4,5-dimethyl-2-thiazolyl)-2,5-diphenyltetrazolium bromide (MTT) assay in HeLa cells. As shown in Figure 6a, no cytotoxicity was found even when HeLa cells were treated with TPE-PNIPAM at the concentration of 200 μg/mL for 48 h. With the characteristic of AIE fluorescence, the TPE-PNIPAM might be used as a fluorescent agent for cellular imaging. As shown in Figure 6b, TPE could be readily detected in HeLa cells after 24 h incubation (the first passage). It was known that conventional fluorophores were rarely retained in the live cells for a long time and extruded to the culture media due to the reverse extra- and intracellular concentration gradient during the passage processes, which made them unsuitable for long-term cellular tracing. To evaluate whether TPE-PNIPAM could be used as a probe to trace the cells long-term, the cells treated with TPE-PNIPAM were repeatedly passaged every 2 days, and the intracellular fluorescence of TPE-PNIPAM in every passage was determined by confocal microscope and flow cytometry. The results showed that the stained cells can retain the strong fluorescence intensities during a long period of 15 days. Over 40% of fluorescence remained for as long as 7 passages (Figure 6c).

DOI: 10.1021/am509161y
ACS Appl. Mater. Interfaces 2015, 7, 3420−3425

These data suggested that TPE-PNIPAM nanoparticles might be an ideal long-term fluorescent cellular tracer.

4. CONCLUSION

In summary, we have developed a novel method for synthesis of TPE-based temperature-sensitive PNIPAM by ATRP. The obtained TPE-PNIPAM can be assembled into fluorescent organic nanoparticles with the size of about 200 nm and with LCST of 34 °C in water. Moreover, the size and fluorescence of the nanoparticles can be tuned by changing temperature. The nanoparticles emitting strong blue-green fluorescence can be readily internalized by HeLa cells with no cytotoxicity and permit the stained cells to be traced for as long as 7 passages. Further research on TPE-PNIPAM in the fields of bioimaging and novel drug-delivery systems is underway.

■ ASSOCIATED CONTENT

Supporting Information

Scheme of synthesis of TPE-PNIPAM, ^{1}H spectrum of **1**, IR spectrum of TPE-PNIPAM, and fluorescent spectra of TPE-PNIPAM in water at different temperature. This material is available free of charge via the Internet at http://pubs.acs.org.

■ AUTHOR INFORMATION

Corresponding Authors

*E-mail: chunzhang@hust.edu.cn.
*E-mail: zhaoyb@hust.edu.cn.
*E-mail: lugan@hust.edu.cn.

Author Contributions

†These authors contributed equally.

Notes

The authors declare no competing financial interest.

■ ACKNOWLEDGMENTS

This work is supported by the National Natural Science Foundation of China (20902031, 81372400, and J1103514), the National Basic Research Program (2012CB932500 and 2015CB931800), the Fundamental Research Funds for the Central Universities (HUST 2013YGYL003), and the Natural Science Foundation of Hubei Province (2013CFB163). We also thank the Analytical and Testing Center of Huazhong University of Science and Technology for related analysis.

■ REFERENCES

(1) Stephens, D. J.; Allan, V. J. Light Microscopy Techniques for Live Cell Imaging. *Science* **2003**, *300*, 82−86.

(2) Swedlow, J. R.; Goldberg, I.; Brauner, E.; Sorger, P. K. Informatics and Quantitative Analysis in Biological Imaging. *Science* **2003**, *300*, 100−102.

(3) Larson, D. R.; Zipfel, W. R.; Williams, R. M.; Clark, S. W.; Bruchez, M. P.; Wise, F. W.; Webb, W. W. Water-Soluble Quantum Dots for Multiphoton Fuorescence Imaging in Vivo. *Science* **2003**, *300*, 1434−1436.

(4) Gao, Y.; Cui, Y.; Chan, J. K.; Xu, C. Stem Sell Tracking With Optically Active Nanoparticles. *Am. J. Nucl. Med. Mol. Imaging* **2013**, *3*, 232−246.

(5) Idris, N. M.; Li, Z. Q.; Ye, L.; Wei, S. E. W.; Mahendran, R.; Ho, P. C. L.; Zhang, Y. Tracking Transplanted Cells in Live Animal Using Upconversion Fluorescent Nanoparticles. *Biomaterials* **2009**, *30*, 5104−5113.

(6) Jaiswal, J. K.; Mattoussi, H.; Mauro, J. M.; Simon, S. M. Long-Term Multiple Color Imaging of Live Cells Using Quantum Dot Bioconjugates. *Nat. Biotechnol.* **2003**, *21*, 47−51.

(7) Yuan, X.; Setyawati, M. I.; Tan, A. S.; Ong, C. N.; Leong, D. T.; Xie, J. Highly Luminescent Silver Nanoclusters with Tunable Emissions: Cyclic Reduction−Decomposition Synthesis and Antimicrobial Properties. *NPG Asia Mater.* **2013**, *5*, e39.

(8) Sutton, E.; Henning, T.; Pichler, B.; Bremer, C.; Daldrup, L. H. Cell Tracking with Optical Imaging. *Eur. J. Radiol.* **2008**, *18*, 2021−2032.

(9) Yang, K.; Li, Z.; Cao, Y.; Yu, X.; Mei, J. Effect of Peptide-Conjugated Near-Infrared Fluorescent Quantum Dots (NIRF-QDs) on the Invasion and Metastasis of Human Tongue Squamous Cell Carcinoma Cell line Tca8113 in Vitro. *Int. J. Mol. Sci.* **2009**, *10*, 4418−4427.

(10) Smith, A. M.; Duan, H.; Mohs, A. M.; Nie, S. M. Bioconjugated Quantum Dots for in Vivo Molecular and Cellular Imaging. *Adv. Drug Delivery Rev.* **2008**, *60*, 1226−1240.

(11) Leung, C. W. T.; Hong, Y.; Chen, S.; Zhao, E.; Lam, J. W.; Tang, B. Z. Photostable AIE Luminogen for Specific Mitochondrial Imaging and Tracking. *J. Am. Chem. Soc.* **2013**, *135*, 62−65.

(12) Shi, H.; Liu, J.; Geng, J.; Tang, B. Z.; Liu, B. Specific Detection of Integrin $\alpha_v\beta_3$ by Light-Up Bioprobe with Aggregation-Induced Emission Characteristics. *J. Am. Chem. Soc.* **2012**, *134*, 9569−9572.

(13) Li, K.; Qin, W.; Ding, D.; Tomczak, N.; Geng, J.; Liu, R.; Liu, J.; Zhang, X.; Liu, H.; Liu, B. Photostable Fluorescent Organic Dots with Aggregation-Induced Emission (AIE Dots) for Noninvasive Long-Term Cell Tracing. *Sci. Rep.* **2013**, *3*, 1150.

(14) Feng, G. X.; Tay, C. Y.; Chui, Q. X.; Liu, R. R.; Tomczak, N.; Liu, J.; Tang, B. Z.; Leong, D. T.; Liu, B. Ultrabright Organic Dots With Aggregation-Induced Emission Characteristics for Cell Tracking. *Biomaterials* **2014**, *35*, 8669−8677.

(15) Yang, H.; Mao, H.; Wan, Z.; Zhu, A.; Guo, M.; Li, Y.; Li, X.; Wan, J.; Yang, X.; Shuai, X.; Chen, H. Micelles Assembled with Carbocyanine Dyes for Theranostic Near-Infrared Fluorescent Cancer Imaging and Photothermal Therapy. *Biomaterials* **2013**, *34*, 9124−9133.

(16) Guo, M.; Mao, H.; Li, Y.; Zhu, A.; He, H.; Yang, H.; Wang, Y.; Tian, X.; Ge, C.; Peng, Q.; Wang, X.; Yang, X.; Chen, X.; Liu, G.; Chen, H. Dual Imaging-Guided Photothermal/Photodynamic Therapy Using Micelles. *Biomaterials* **2014**, *35*, 4656−4666.

(17) Zhang, C.; Liu, Y.; Xiong, X.-Q.; Peng, L.-H.; Gan, L.; Chen, C.-F.; Xu, H.-B. Three-Dimensional Nanographene Based on Triptycene: Synthesis and Its Application in Fluorescence Imaging. *Org. Lett.* **2012**, *14*, 5912−5915.

(18) Birks, J. B. *Photophysics of Aromatic Molecules*. Wiley-Interscience: London, 1970.

(19) Luo, J. D.; Xie, Z. L.; Lam, J. W. Y.; Cheng, L.; Chen, H. Y.; Qiu, C. F.; Kwok, H. S.; Zhan, X. W.; Liu, Y. Q.; Zhu, D. B.; Tang, B. Z. Aggregation-Induced Emission of 1-Methyl-1,2,3,4,5-pentaphenylsilole. *Chem. Commun.* **2001**, *18*, 1740−1741.

(20) Hong, Y.; Lam, J. W. Y.; Tang, B. Z. Aggregation-Induced Emission. *Chem. Soc.Rev.* **2011**, *40*, 5361−5388.

(21) Hong, Y.; Lam, J. W. Y.; Hong, Y.; Lam, J. W. Y.; Tang, B. Z. Aggregation-Induced Emission: Phenomenon, Mechanism and Applications. *Chem. Commun.* **2009**, *29*, 4332−4353.

(22) Chen, Q.; Zhang, D. Q.; Zhang, G.-X.; Yang, X. Y.; Feng, Y.; Fan, Q. H.; Zhu, D. B. Multicolor Tunable Emission from Organogels Containing Tetraphenylethene, Perylenediimide, and Spiropyran Derivatives. *Adv. Funct. Mater.* **2010**, *19*, 3244−3251.

(23) Huang, G.; Ma, B.; Chen, J.; Peng, Q.; Zhang, G. X.; Fan, Q.; Zhang, D. Q. Dendron-Containing Tetraphenylethylene Compounds: Dependence of Fluorescence and Photocyclization Reactivity on the Dendron Generation. *Chem.—Eur. J.* **2012**, *18*, 3886−3892.

(24) Gu, X.-G.; Yao, J. J.; Zhang, G.-X.; Zhang, C.; Yan, Y. L.; Zhao, Y. S.; Zhang, D. Q. New Electron-Donor/Acceptor-Substituted Tetraphenylethylenes: Aggregation-Induced Emission with Tunable Emission Color and Optical-Waveguide Behavior. *Chem.—Asian J.* **2013**, *8*, 2362−2369.

(25) Liu, Y.; Deng, C. M.; Tang, L.; Qin, A.-J.; Hu, R.-R.; Sun, J.-Z.; Tang, B. Z. Specific Detection of D-Glucose by a Tetraphenylethene-Based Fluorescent Sensor. *J. Am. Chem. Soc.* **2011**, *133*, 660−663.

DOI: 10.1021/am509161y
ACS Appl. Mater. Interfaces 2015, 7, 3420−3425

(26) Gu, X. G.; Zhang, G. X.; Wang, Z.; Liu, W. W.; Xiao, L.; Zhang, D. Q. A New Fluorometric Turn-on Assay for Alkaline Phosphatase and Inhibitor Screening Based on Aggregation and Deaggregation of Tetraphenylethylene Molecules. *Analyst.* **2013**, *138*, 2427−2431.
(27) Liu, N.-N.; Song, S.; Li, D. M.; Zheng, Y. S. Highly Sensitive Determination of Enantiomeric Composition of Chiral Acids Based on Aggregation-Induced Emission. *Chem. Commun.* **2012**, *48*, 4908−4910.
(28) Feng, H. T.; Zheng, Y. S. Highly Sensitive and Selective Detection of Nitrophenolic Explosives by Using Nanospheres of a Tetraphenylethylene Macrocycle Displaying Aggregation-Induced Emission. *Chem.—Eur. J.* **2014**, *20*, 195−201.
(29) Feng, H. T.; Zheng, Y. S. Self-Assembled Tetraphenylethylene Macrocycle Nanofibrous Materials for the Visual Detection of Copper(II) in Water. *J. Mater. Chem. C* **2014**, *2*, 2353−2359.
(30) Zhang, M.; Feng, G. X.; Song, Z. G.; Zhou, Y. P.; Chao, H. Y.; Yuan, D. Q.; Tan, T. T. Y.; Guo, Z. G.; Hu, Z. G.; Tang, B. Z.; Liu, B.; Zhao, D. Two-Dimensional Metal−Organic Framework with Wide Channels and Responsive Turn-On Fluorescence for the Chemical Sensing of Volatile Organic Compounds. *J. Am. Chem. Soc.* **2014**, *136*, 7241−7244.
(31) Zhang, C.; Wang, Z.; Song, S.; Zheng, Y. S.; Yang, X. L.; Xu, H. B. Tetraphenylethylene-Based Expanded Oxacalix-Arene: Synthesis, Structure, and Its Supramolecular Grid Assemblies Directed by Guests in the Solid State. *J. Org. Chem.* **2014**, *79*, 2729−2732.
(32) Wang, Z. K.; Chen, S. J.; Lam, J. W. Y.; Qin, W.; Kwok, R. T. K.; Xie, N.; Hu, Q. L.; Tang, B. Z. Long-Term Fluorescent Cellular Tracing by the Aggregates of AIE Bioconjugates. *J. Am. Chem. Soc.* **2013**, *135*, 8238−8245.
(33) Li, M.; Hong, Y. N.; Wang, Z. K.; Chen, S. J.; Gao, M.; Kwok, R. T. K.; Qin, W.; Lam, J. W. Y.; Zheng, Q. C.; Tang, B. Z. Fabrication of Chitosan Nanoparticles with Aggregation-Induced Emission Characteristics and Their Applications in Long-Term Live Cell Imaging. *Macromol. Rapid Commun.* **2013**, *34*, 767−771.
(34) Zhang, X. Y.; Zhang, X. Q.; Yang, B.; Liu, M. Y.; Liu, W. Y.; Chen, Y. W.; Wei, Y. Facile Fabrication and Cell Imaging Applications of Aggregation-Induced Emission Dye-Based Fluorescent Organic Nanoparticles. *Polym. Chem.* **2013**, *4*, 4317−4321.
(35) Yallapu, M. M.; Jaggi, M.; Chauhan, S. C. Design and Engineering of Nanogels for Cancer Treatment. *Drug Discovery Today* **2011**, *16*, 457−463.
(36) Saunders, B. R.; Laajam, N.; Daly, E.; Teow, S.; Hu, X.; Stepto, R. Microgels: From Responsive Polymer Colloids to Biomaterials. *Adv. Colloid Interface Sci.* **2009**, *147−148*, 251−262.
(37) Blackburn, W. H.; Dickerson, E. B.; Smith, M. H.; McDonald, J. F.; Lyon, L. A. Peptide-Functionalized Nanogels for Targeted siRNA Delivery. *Bioconjugate Chem.* **2009**, *20*, 960−968.
(38) Zhou, Y. M.; Ishikawa, A.; Okahashi, R.; Uchida, K.; Nemoto, Y.; Nakayama, M.; Nakayama, Y. Deposition Transfection Technology Using a DNA Complex with a Thermoresponsive Cationic Star Polymer. *J. Controlled Release* **2007**, *123*, 239−246.
(39) Hong, S. W.; Kim, D. Y.; Lee, J. U.; Jo, W. H. Synthesis of Polymeric Temperature Sensor Based on Photophysical Property of Fullerene and Thermal Sensitivity of Poly(*N*-isopropylacrylamide). *Macromolecules* **2009**, *42*, 2756−2761.
(40) Chen, H.; Zhu, H.; Hu, J.; Zhao, Y.; Wang, Q.; Wan, J.; Yang, Y. J.; Xu, H. B.; Yang, X. L. Highly Compressed Assembly of Deformable Nanogels into Nanoscale Suprastructures and Their Application in Nanomedicine. *ACS Nano* **2011**, *5*, 2671−2680.
(41) Xiong, W.; Gao, X.; Zhao, Y.; Xu, H.; Yang, X. The Dual Temperature/pH-Sensitive Multiphase Behavior of Poly(*N*-isopropylacrylamide-co-acrylic acid) Micro-Gels for Potential Application in In Situ Gelling System. *Colloids Surf, B* **2011**, *84*, 103−110.
(42) Xiong, W.; Wang, W.; Wang, Y.; Zhao, Y. B.; Chen, H. B.; Xu, H. B.; Yang, X. L. Dual Temperature/pH-Sensitive Drug Delivery of Poly(*N*-isopropylacrylamide-co-acrylic acid) Nanogels Conjugated with Doxorubicin for Potential Application in Tumor Hyperthermia Therapy. *Colloids Surf, B* **2011**, *84*, 447−453.
(43) Zhao, Y. B.; Zheng, C. S.; Wang, Q.; Fang, J. L.; Zhou, G. F.; Zhao, H.; Yang, Y. J.; Xu, H. B.; Feng, G. S.; Yang, X. L. Permanent and Peripheral Embolization: Temperature-Sensitive p(*N*-Isopropylacrylamide-co-butyl methylacrylate) Nanogel as a Novel Blood-Vessel-Embolic Material in the Interventional Therapy of Liver Tumors. *Adv. Funct Mater.* **2011**, *21*, 2035−2042.
(44) Jiang, L. Y.; Zhou, Q.; Mu, K. T.; Xie, H.; Zhu, Y. H.; Zhu, W. Z.; Zhao, Y. B.; Xu, H. B.; Yang, X. L. pH/Temperature Sensitive Magnetic Nanogels Conjugated with Cy5.5-Labled Lactoferrin for MR and Fluorescence Imaging of Glioma in Rats. *Biomaterials* **2013**, *34*, 7418−7428.
(45) Tang, L.; Jin, J. K.; Qin, A. J.; Yuan, W. Z.; Mao, Y.; Mei, J.; Sun, J. Z.; Tang, B. Z. A Fluorescent Thermometer Operating in Aggregation-Induced Emission Mechanism: Probing Thermal Transitions of PNIPAM in Water. *Chem. Commun.* **2009**, *33*, 4974−4976.

DOI: 10.1021/am509161y
ACS Appl. Mater. Interfaces 2015, 7, 3420−3425